JACS
JOURNAL OF THE AMERICAN CHEMICAL SOCIETY
Article
pubs.acs.org/JACS

Associative Interactions in Crowded Solutions of Biopolymers Counteract Depletion Effects

Joost Groen,[†] David Foschepoth,[†] Esra te Brinke,[†] Arnold J. Boersma,[‡] Hiromi Imamura,[§] Germán Rivas,[⊥] Hans A. Heus,[†] and Wilhelm T. S. Huck*[,†]

[†]Institute for Molecules and Materials, Radboud University, 6525 AJ, Nijmegen, The Netherlands
[‡]Groningen Biomolecular Sciences and Biotechnology Institute, University of Groningen, 9747 AG Groningen, The Netherlands
[§]Graduate School of Biostudies & The Hakubi Center for Advanced Research, Kyoto University, 606-8501 Kyoto, Japan
[⊥]Centro de Investigaciones Biológicas, CSIC, C/Ramiro de Maeztu 9, E-40 28040 Madrid, Spain

Supporting Information

ABSTRACT: The cytosol of *Escherichia coli* is an extremely crowded environment, containing high concentrations of biopolymers which occupy 20−30% of the available volume. Such conditions are expected to yield depletion forces, which strongly promote macromolecular complexation. However, crowded macromolecule solutions, like the cytosol, are very prone to nonspecific associative interactions that can potentially counteract depletion. It remains unclear how the cytosol balances these opposing interactions. We used a FRET-based probe to systematically study depletion in vitro in different crowded environments, including a cytosolic mimic, *E. coli* lysate. We also studied bundle formation of FtsZ protofilaments under identical crowded conditions as a probe for depletion interactions at much larger overlap volumes of the probe molecule. The FRET probe showed a more compact conformation in synthetic crowding agents, suggesting strong depletion interactions. However, depletion was completely negated in cell lysate and other protein crowding agents, where the FRET probe even occupied slightly more volume. In contrast, bundle formation of FtsZ protofilaments proceeded as readily in *E. coli* lysate and other protein solutions as in synthetic crowding agents. Our experimental results and model suggest that, in crowded biopolymer solutions, associative interactions counterbalance depletion forces for small macromolecules. Furthermore, the net effects of macromolecular crowding will be dependent on both the size of the macromolecule and its associative interactions with the crowded background.

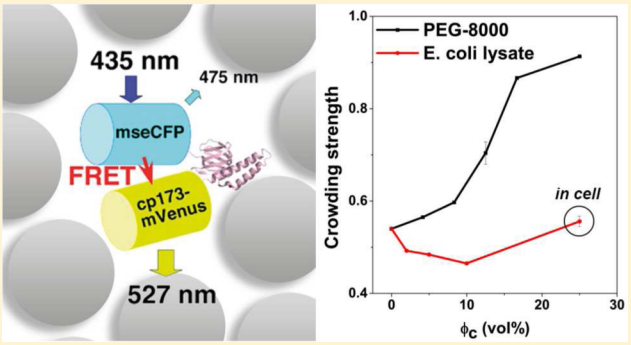

INTRODUCTION

The cytosol of *Escherichia coli* consists of a complex, crowded solution of biopolymers which occupy 20−30 vol %.[1,2] This environment leads to strongly reduced and nonrandom diffusion of macromolecules[3,4] and is also expected to yield increased thermodynamic activities due to significant volume occupation.[5] Moreover, repulsive interactions of macromolecules with the background macromolecules will favor associations and compact conformations of molecules as a result of depletion interactions.[6,7] When two macromolecules come in close enough proximity for their hard-core excluded volumes to overlap, the total excluded volume of the two molecules is reduced because of this overlap volume. As background macromolecules are excluded from the space between the two molecules in this situation, there is a difference in the concentration of background macromolecules outside the two molecules and in the interstitial space. This generates an anisotropic osmotic pressure which pushes the molecules together. The resulting force is called the depletion force.[8]

Exactly how the physicochemical properties of the crowded cytosol affect key biochemical processes in the cell is unknown. The effects of macromolecular crowding on biochemical reactions are typically studied in vitro by the addition of high concentrations of inert, synthetic polymers such as polyethylene glycol (PEG), Ficoll, or dextran. Such studies have found a significant hard-core excluded volume effect (colloquially shortened to excluded volume effect), resulting in increased association constants and rates,[9−15] increased protein stability,[16−20] and increased aggregation.[21−23]

However, whether high concentrations of inert, uncharged synthetic polymers can faithfully mimic cytosolic conditions is questionable. The cytosolic environment is dominated by proteins of different shapes, size, and charge. The differences between this environment and a solution of inert polymers have been noted and illustrated previously.[24] The heterogeneous cytosol is replete with nonspecific chemical interactions, both

Received: July 28, 2015
Published: September 18, 2015

DOI: 10.1021/jacs.5b07898
J. Am. Chem. Soc. 2015, 137, 13041−13048

associative and repulsive, whereas in synthetic crowding agents steric repulsion dominates. This means that in crowded biopolymer solutions such as the cytosol, the crowded environment cannot be considered chemically inert. In these environments, chemical interactions of all macromolecules, including the crowded environment, need to be considered in addition to excluded volume effects. In short, macromolecular crowding has an enthalpic component (chemical interactions) that needs to be considered in addition to its well-established entropic effects. A computational study by McGuffee and Elcock first predicted that homodimeric complexation of proteins resulting from depletion interactions "is largely cancelled by the more favorable energetic interactions that the monomers form with the cytoplasm constituents."[25] Subsequent experimental work has also postulated that these chemical, associative interactions are responsible for attenuation of excluded volume effects in crowded biopolymer solutions.[26−28] In addition, chemical interactions were included in existing theoretical models of macromolecular crowding.[29,30]

It remains unclear how depletion interactions and associative chemical interactions are balanced in crowded biopolymer solutions such as the cytosol, and how these interactions scale with the size of the probe macromolecule. Therefore, there is an urgent need for better model systems that allow for systematic studies of the effects of macromolecular crowding in a cytosolic mimic using different crowding agents and specially designed crowding probes.

A number of studies have used *E. coli* lysate to mimic cytosolic conditions.[26,31] We prepared an *E. coli* lysate where both the periplasmic and membrane fractions are removed (as these are not part of the native cytosol), to study the effects of macromolecular crowding in vitro. After dialysis and lyophilization, this lysate can be reconstituted to clear solutions of high concentration (∼10 vol % macromolecules). We studied the effects of macromolecular crowding in synthetic crowding agents (PEG-8000 and Ficoll 70), protein-based crowding agents (BSA and ovomucoid), and our *E. coli* lysate to compare the effects of different crowded environments.

We used an ATP FRET sensor as a crowding probe to study depletion effects in vitro, analogous to two recent studies.[32,33] Our in vitro approach allows us to probe the depletion and chemical interactions that jointly result in a net crowding effect. We hypothesized that the previously engineered ATP FRET sensor[34] (AT1.03, hereafter called ATeam) and an ATP-insensitive version of this sensor (AT1.03$^{R122\ K/R126\ K}$, hereafter called DTeam for dummy ATeam) will both be sensitive to depletion interactions, as compact conformations of these probes should increase their FRET efficiency significantly as depicted in Figure 1. Moreover, because the starting FRET efficiency of these probes in dilute solution is more favorable (around 0.5) than FRET constructs used in previous studies, we hypothesized ATeam and DTeam would be more sensitive to depletion effects.

In parallel, we studied bundle formation of FtsZ protofilaments as a probe for macromolecular interactions at larger overlap volumes. FtsZ is a protein (hydrodynamic radius of 5 nm)[35] involved in cell division, that assembles into a ring of FtsZ filaments called the Z-ring.[36−38] Upon binding of GTP, FtsZ polymerizes in vitro to form long protofilaments (∼200 nm) with a diameter of 5 nm.[39] These protofilaments have been reported to assemble into bundles and fibers and the formation of these higher order structures have been investigated in vitro in microdroplets.[40] By approximating an FtsZ protofilament with a rectangular cuboid, we calculate that the overlap volume of two FtsZ protofilaments is ∼15× larger than the overlap volume of the FRET probe (Figure S1).

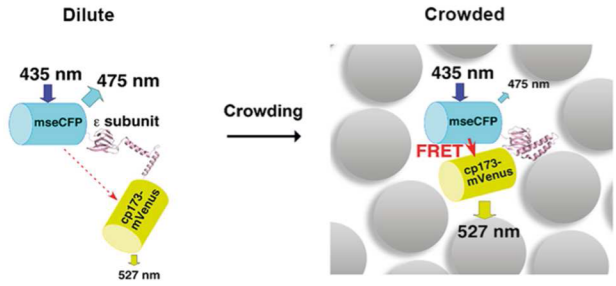

Figure 1. Promotion of a more compact conformation of a FRET probe by depletion interactions induces an increase in FRET efficiency. Adapted from Imamura et al. 2009.[34]

In this study, we report the net crowding effects, using two depletion probes of different sizes, of differently crowded environments: two synthetic crowding agents, two protein crowding agents and an *E. coli* lysate to approximate cytosolic conditions. By using two depletion probes of different sizes we can study depletion forces at two different size scales, assuming the propensity for associative interactions of these probes is identical. This allows us to determine the relative contributions of depletion interactions and associative interactions to the resultant net effects of macromolecular crowding.

RESULTS

Effects of Macromolecular Crowding on FRET-Based Probes. We studied two variants of an ATP-sensor called ATeam,[34] one with a K_d in the low-millimolar range (ATeam) and a mutant insensitive to ATP (DTeam). To approach physiological conditions, measurements were performed in physiological salt solutions and at 37 °C. To study the effects of macromolecular crowding on ATeam and DTeam FRET efficiencies, we measured the YFP/CFP emissions (527/475 nm) of these probes under crowded conditions in the absence of ATP using 430 nm excitation wavelength. FRET efficiency is defined as FRET = $(I_A/(I_D + I_A))$ where I_A and I_D are acceptor and donor emission intensities, respectively.

Volume fractions of crowding agents were calculated from mass concentrations and partial specific volumes (Table S1). Figure 2 shows FRET efficiencies for a concentration range of different crowding agents. Synthetic crowding agents PEG-8000 (25 vol %) and Ficoll 70 (20 vol %) strongly increased FRET efficiency of DTeam from 0.54 ± 0.01 to 0.91 ± 0.01 and 0.70 ± 0.02, respectively. PEG-8000 (25 vol %) and Ficoll 70 (20 vol %) changed the FRET efficiency of ATeam from 0.55 ± 0.01 to 0.87 ± 0.02 and 0.72 ± 0.04, respectively. As ATeam and DTeam respond similarly to crowded conditions, DTeam was used in subsequent experiments, as it is insensitive to ATP concentrations.

In contrast to synthetic crowding agents, BSA and ovomucoid slightly decrease the FRET efficiency of these probes, with some recovery at higher volume fractions. Cell-free *E. coli* lysate lowered the FRET efficiency of the DTeam probe with increasing lysate concentration to an even larger extent than BSA and ovomucoid: from 0.54 ± 0.01 to 0.47 ± 0.01 at 10 vol % lysate.

We also measured the FRET efficiency of DTeam in *E. coli* culture and determined a FRET efficiency in cell of 0.56 ± 0.01

DOI: 10.1021/jacs.5b07898
J. Am. Chem. Soc. 2015, 137, 13041−13048

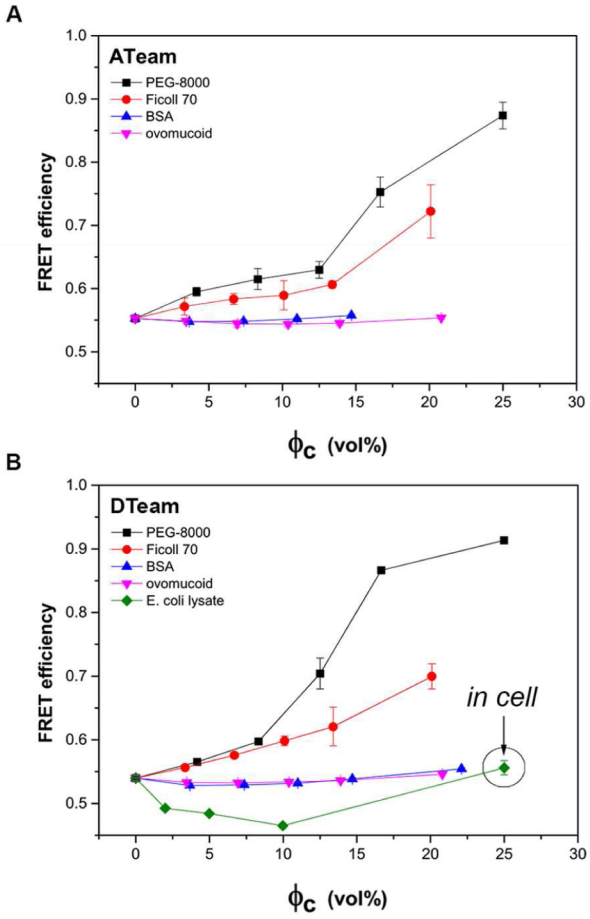

Figure 2. (A) FRET efficiencies of the ATeam probe in different crowded conditions at 37 °C. (B) FRET efficiencies of the DTeam probe in different crowded conditions at 37 °C. In cell measurements of DTeam in *E. coli* at 37 °C was included as data point at 25 vol % *E. coli* lysate. Error bars denote standard deviations.

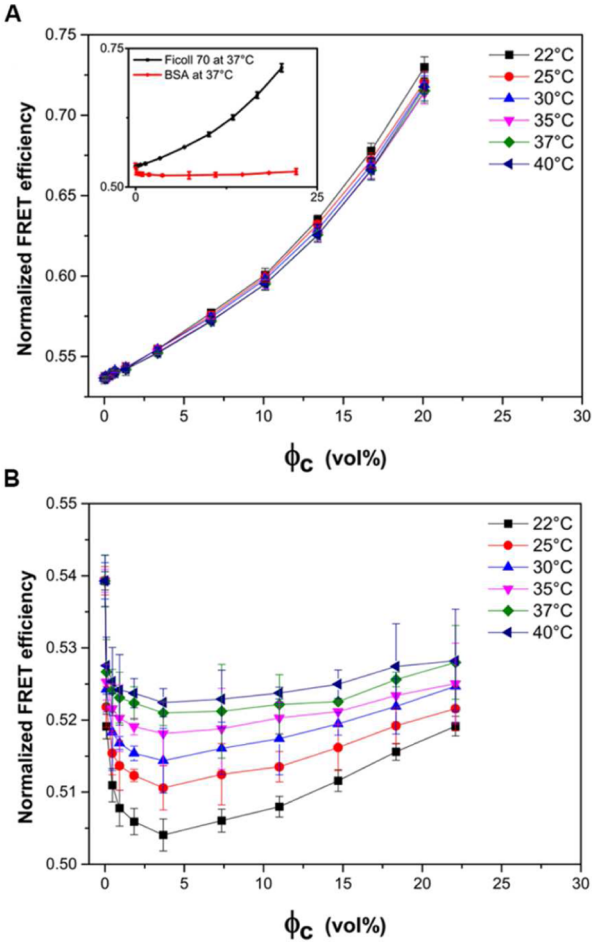

Figure 3. Temperature dependence of FRET efficiencies of DTeam. Data corrected for temperature induced FRET efficiency changes in the absence of crowding agent. (A) DTeam probe in Ficoll 70 solutions at different temperatures. Inset shows DTeam probe in Ficoll 70 (green trace Figure 3A) and BSA solutions (green trace Figure 3B) at 37 °C. (B) DTeam probe in BSA solutions at different temperatures. Error bars denote standard deviations.

compared to 0.54 ± 0.01 in dilute solution (Supporting Information (SI) Materials and Methods).

Temperature Effects on Net Crowding Effects in Different Crowded Environments. Subsequently, we tested FRET efficiencies of DTeam at different temperatures to determine the effects of temperature on depletion and associative interactions.

Figure 3 shows measurements of DTeam in Ficoll 70 and BSA solutions at different temperatures. Measurements were corrected for the effects of temperature on FRET efficiencies in the absence of crowding agent. Ficoll 70 and BSA were selected because they have similar molecular weight and size.

We observe no significant effect of temperature on FRET efficiencies in Ficoll 70 solutions, suggesting depletion interactions are relatively unperturbed by temperature changes in the range used.

FRET measurements in BSA show a different trend (Figure 3B): at low volume fractions, the presence of crowding agent generates a significant dip in FRET efficiency, whereas at higher volume fractions the FRET efficiency recovers almost completely. In the case of BSA, an increase in temperature counteract the initial dip in FRET efficiency at low volume occupancies and had a smaller effect at higher crowding agent volume fractions although it maintained the trend observed at lower temperatures.

Bundle Formation of FtsZ Induced by Depletion Interactions. To probe the effects of macromolecular crowding at high overlap volumes, we studied FtsZ bundle formation under crowded conditions similar to those used in the FRET experments. FtsZ protofilaments are ∼5 nm in diameter and thus droplets containing only protofilaments appear homogeneous in fluorescence.

These protofilaments can form bundles by depletion forces and these bundles are large enough to be visualized using conventional confocal microscopy (Figure 4A). We investigated the effects of different crowded environments on FtsZ bundle formation by encapsulating the components (buffer, GTP, FtsZ and crowding agent) in microdroplets using microfluidic devices (Figure 4B). Osmotic shrinkage of the droplets was used to gradually concentrate the droplet's contents and subsequently bundle formation of FtsZ was followed by confocal microscopy.

Figure 4 shows FtsZ bundle formation using crowding agents at different concentrations. In the absence of crowding agent, fluorescence in droplets is homogeneous (no bundle formation) even after concentrating the droplet contents 2.5× by shrinkage. Droplet shrinkage in subsequent experiments with crowding agent was never greater than ∼2× in volume

DOI: 10.1021/jacs.5b07898
J. Am. Chem. Soc. 2015, 137, 13041−13048

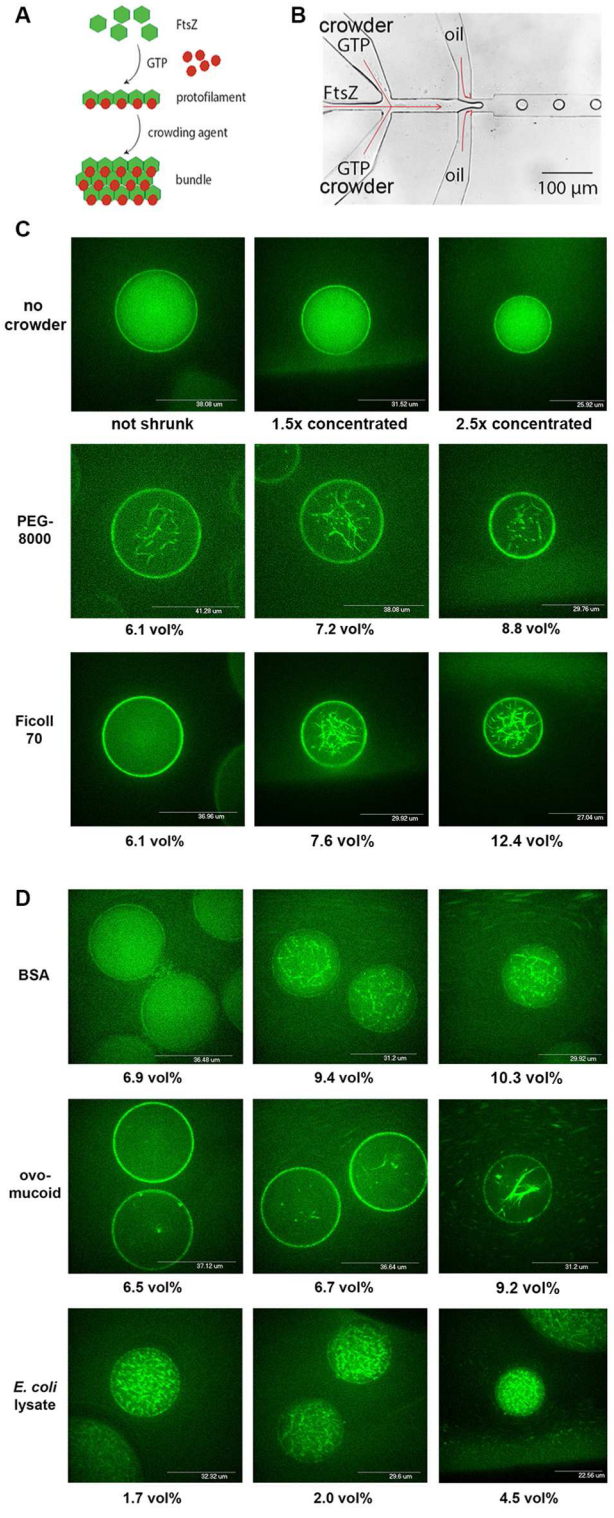

Figure 4. FtsZ bundle formation in microdroplets under different crowded conditions. (A) FtsZ forms protofilaments by binding GTP. Depletion interactions generated by macromolecular crowding can bundle these filaments. (B) Microfluidic setup. A mixture of GTP and crowding agent is mixed on-chip with an FtsZ solution and microdroplets are generated subsequently. (C) FtsZ bundle formation without crowding agent and with polymeric crowding agents PEG-8000 and Ficoll 70. (D) Bundle formation of FtsZ with protein-based crowding agents BSA, ovomucoid, and *E. coli* lysate. 1% of FtsZ molecules is labeled with Alexa-488. Panels (A) and (B) adapted from Mellouli et al. 2013.[40]

reduction. PEG-8000 produced bundles without any droplet shrinkage, which shows it has the largest depletion effect. Ficoll 70 shows clear bundle formation at 7.6 vol % crowding agent. Surprisingly, both BSA and ovomucoid were able to induce FtsZ bundle formation at ∼9 and ∼7.5 vol %, respectively. FtsZ also showed strong bundle formation in *E. coli* lysate.

■ DISCUSSION

Macromolecular crowding is expected to lead to more compact conformations of macromolecules because of excluded volume effects. We used an in vitro approach to systematically study the effects of different crowded environments on probes of different sizes, both of which are sensitive to depletion interactions. We also used an *E. coli* lysate as a crowding medium. This lysate can be dissolved to high concentrations (10 vol %) to approximate cytosolic conditions, be it at lower concentrations than present in the cell.

We tested the FRET efficiencies of two versions of a genetically encoded ATP sensor in different crowding media and found that these FRET constructs are indeed sensitive to macromolecular crowding. As hypothesized, they are much more sensitive than previously developed FRET crowding probes.[32,33] Commonly used synthetic crowding agents PEG-8000 and Ficoll 70 strongly promoted more compact FRET probe conformations (higher FRET efficiencies), while protein-based crowding agents BSA and ovomucoid show an initial dip in FRET at low crowding agent concentrations, with slight recovery at higher concentrations. These results suggest that, even at low concentrations, associative interactions of the protein crowding agents with the FRET probes can promote a more open conformation of the probe. However, both BSA and ovomucoid show recovery of FRET efficiency at higher volume fractions. This indicates that, at a critical point, depletion interactions start to counteract associative interactions and promote more compact conformations of the probe. However, even at very high volume fractions of BSA and ovomucoid, the FRET probes do not completely recover to the FRET efficiencies they have in dilute solutions.

Notably, measurements in *E. coli* lysate showed the greatest reduction in FRET efficiency, going from 0.54 in buffer to 0.47 at 10 vol % lysate. It is possible that *E. coli* lysate will show a recovery of probe FRET efficiency at higher volume fractions, like BSA and ovomucoid, but we are not able to concentrate the lysate to more than 10 vol %. We therefore measured the FRET efficiency of DTeam in cell in bacterial culture and indeed see that at crowded conditions present in cells, the FRET efficiency of DTeam (0.56 ± 0.01) is similar to dilute conditions (0.54 ± 0.01).

In line with the computational results of McGuffee and Elcock, we observe that the depletion interaction of two macromolecules in the cytosol by macromolecular crowding is canceled out by associative interactions with the crowded background.[25] Of particular importance is also the fact that these observations agree with in cell experiments reported previously: measurements of ATeam in *E. coli* show FRET efficiencies lower than those measured in buffer when ATP production was stopped by the addition of 40 mM KCN.[41] Moreover, Imamura et al. reported no changes in FRET efficiencies when DTeam was targeted to different organelles (cytoplasm, nucleus, and mitochondria) in HeLa cells: the reported FRET efficiencies in cell were not significantly different from those measured in buffer solution.[34] This implies that, on the level of the FRET probes, there is no net depletion

DOI: 10.1021/jacs.5b07898
J. Am. Chem. Soc. 2015, 137, 13041−13048

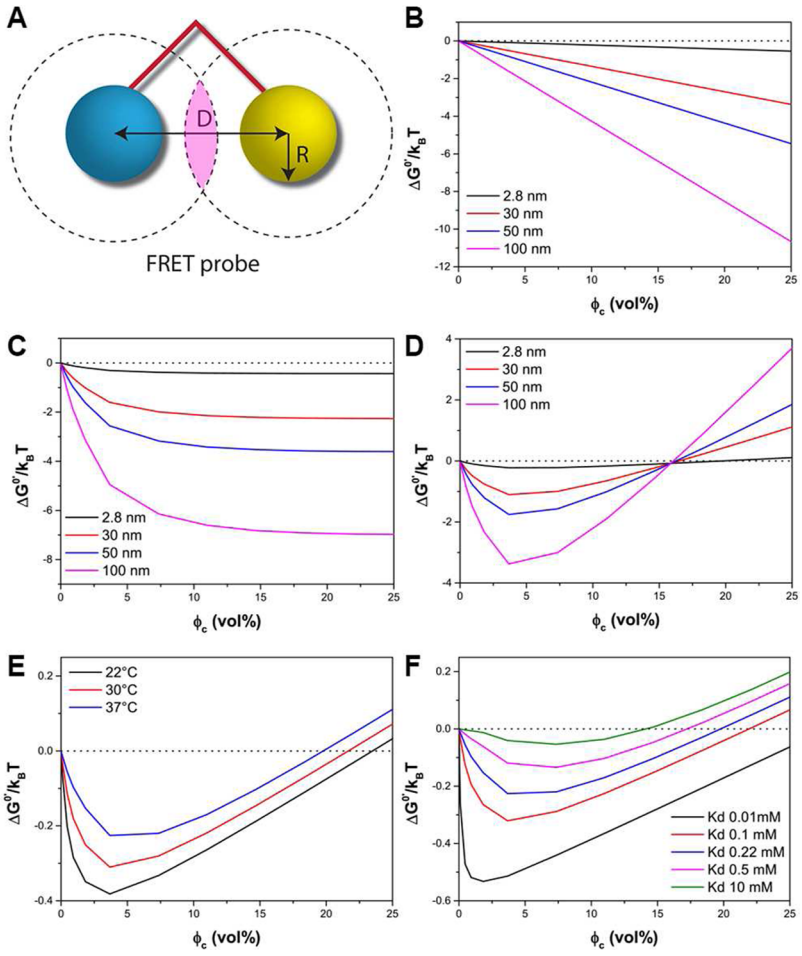

Figure 5. Model predictions of free energy values of depletion, associative interactions. BSA was taken as a crowding agent at different volume fractions (Φ_c). (A) Representation of DTeam FRET probe for depletion. Dotted circles represent hard-core excluded volume and magenta area denotes overlap volume. (B) $\Delta G^{0\prime}_{\text{depletion}}$ calculated for different probe radii (nm). (C) $\Delta G^{0\prime}_{\text{penalty}}$ calculated for different probe radii (nm). (D) $\Delta G^{0\prime}_{\text{eff}}$ calculated for different probe radii. (E) Model predictions for free energies of 2.8 nm radius probe molecule at different temperatures (295, 303, and 310 K). (F) Calculations of $\Delta G^{0\prime}_{\text{eff}}$ for different binding site dissociation constants for a 2.8 nm radius probe molecule.

effect in HeLa cells, not even in mitochondria which are known to have an extremely crowded interior.[42] Our in cell measurement also fits in vivo measurements on protein stability, where the crowded in vivo environment did not provide a substantial stability increase by excluded volume effects.[43−45] Moreover, our results are also in line with NMR experiments on protein stability in *E. coli* cell lysate,[26] which showed slight destabilization op protein folds in BSA and cell lysate but stabilization in Ficoll 70.

The in vitro approach reported here allows us to vary the temperature and study the effects on the FRET crowding probe. We decided to study the DTeam probe in Ficoll 70 and BSA solutions to investigate the temperature dependency of associative and depletion interactions to discriminate depletion interactions and associative interactions. Ficoll 70 and BSA were chosen because they are a synthetic and protein based crowding agent with similar molecular weights. FRET efficiencies of DTeam in Ficoll 70 did not change with temperature, suggesting depletion interactions are not significantly affected by temperature in the range we studied. In contrast, FRET efficiencies in BSA solutions show a significant temperature dependency. The initial dip in FRET efficiency at low crowding agent concentrations is significantly larger at lower temperatures, indicating that associative interactions are affected by temperature, which follows logically from the fact that the Gibbs free energy of binding is temperature dependent. Interestingly, the FRET efficiency is less affected by temperature under highly crowded conditions (20 vol %).

To check how depletion interactions and associative interactions scale with probe size, we also studied a crowding sensitive system with much larger overlap volumes, FtsZ, under different crowded conditions in microdroplets. FtsZ protofilaments can form bundles as a result of depletion interactions, generating structures that can be visualized by confocal microscopy. Because FtsZ protofilaments have a much larger overlap volume than the YFP/CFP fluorescent proteins of FRET probes, we hypothesized that these structures would be subject to much larger depletion interactions under the same crowded conditions. As established previously in microdroplets,[40] indeed synthetic crowding agents can generate depletion interactions sufficient for FtsZ bundle formation.

Interestingly, we found that conditions that decrease FRET efficiencies of the FRET probes were able to significantly promote bundle formation of FtsZ protofilaments. Crowding by *E. coli* lysate, BSA, and ovomucoid led to a slight decrease of FRET efficiency of DTeam at 10 vol %, indicating a more open conformation of the probe. Under the same crowded conditions, lysate, BSA, and ovomucoid induced strong bundle

DOI: 10.1021/jacs.5b07898
J. Am. Chem. Soc. 2015, 137, 13041−13048

formation of FtsZ protofilaments, indicating a strong net depletion interaction. Since FtsZ is an endogenous *E. coli* protein, we cannot exclude the possibility that factors present in the lysate affect FtsZ bundle formation to a certain extent. In short, our results indicate that macromolecular crowding in dense macromolecule solutions, as present in the cytosol, can indeed generate depletion interactions. However, at low overlap volumes these can apparently be overcome by chemical, associative interactions to yield no net crowding effect.

To explain our experimental results, we constructed a model showing the balance of free energy values of depletion interactions and associative interactions. (SI Materials and Methods) For depletion interactions, we use the full AO model[6,8] to calculate free energy values using the following function:

$$\Delta G^{0'}_{\text{depletion}} = -\left(1 + \frac{3}{2\left(\frac{R}{r}\right)}\right)\phi k_B T$$

Where R is the radius of the probe particle, r the radius of the crowding agent, φ the volume fraction of crowding agent, k_B the Boltzmann constant, and T temperature in Kelvin. In this derivation, we use BSA as a crowding agent for our model (r = 3.6 nm).

For the associative interactions, we base our model on NMR measurements of nonspecific interactions of Ca^{2+}-calmodulin with the background molecules in *E. coli* lysate.[46] This work provides a dissociation constant for the associative interaction (K_D = 0.22 mM) which we use in this model. Taking into account the Stokes radius of Ca^{2+}-calmodulin (2.4 nm),[47] we can approximate Ca^{2+}-calmodulin as a sphere with a surface area of 72 nm^2. The starting point of our model is therefore 1 binding site every 72 nm^2 with a K_D of 0.22 mM. As we will show below, our model can easily simulate the effects of stronger or weaker associative interactions.

$$\Delta G^{0'}_{\text{association}} = k_B T \ln(K_D)$$

The dissociation constant corresponds to a strength of the interaction of 5.2 kcal/mol, which is equivalent to 2−3 peptide hydrogen bonds in solution.[48] Binding sites are taken to be homogeneously distributed over the surface of the probe. Thermodynamic activity coefficients resulting from excluded volume effects (γ_{exvol}) were taken into account and calculated as described by Minton in 2013.[29]

$$\text{fraction bound: } \nu = \frac{([A]\gamma_{\text{exvol}})}{K_D + ([A]\gamma_{\text{exvol}})}$$

When two probe molecules come into close proximity, the overlap volume effectively buries surface area of both probe molecules, which subsequently is unavailable for associative chemical interactions with the crowding agent. This buried surface yields a free energy penalty which counteracts the depletion interaction. We calculate the buried surface (A_b) by calculating the surface area of the two spherical caps that form the overlap volume (Figure 5A and SI Materials and Methods). The number of buried binding sites, N_b, is then

$$N_b = A_b \rho_a$$

where ρ_A is the number of binding sites per square nanometer of probe. The density of binding sites is set to 1 binding site every 72 nm^2 of probe surface (ρ_A = 13.9 × 10^{-3}/nm^2), meaning that, for example, a BSA molecule (hydrodynamic radius of 3.6 nm) would have ∼2 binding sites for macromolecules of the same size.

Combining this with the bound fraction (ν), we obtain a free energy penalty of

$$\Delta G^{0'}_{\text{penalty}} = \nu N_b \Delta G^{0'}_{\text{association}}$$

The effective free energy ($\Delta G^{0\prime}_{\text{eff}}$) is calculated by balancing $\Delta G^{0\prime}_{\text{depletion}}$ and $\Delta G^{0\prime}_{\text{penalty}}$.

$$\Delta G^{0'}_{\text{eff}} = \Delta G^{0'}_{\text{penalty}} - \Delta G^{0'}_{\text{depletion}}$$

$$\Delta G^{0'}_{\text{eff}}(R) = k_B T\left(\nu N_b \ln K_D - \left(1 + \frac{3}{2}\frac{r}{R}\right)\phi\right)$$

A positive value for $\Delta G^{0\prime}_{\text{eff}}$ represents a net depletion force while a negative value represents chemical, associative interactions with the background macromolecules overcoming depletion interactions. Figure 5B−D shows the model predictions for free energies of depletion and associative interactions for probe molecules of 2.8, 30, 50, and 100 nm radius. In addition, Figure 5E shows the effective free energy prediction of two 2.8 nm radius probe particles (hydrodynamic radius of GFP) at different temperatures. To provide an estimate of the effects different interaction strengths might have, we plot in Figure 5F energy changes for associative interactions with different dissociation constants. These predictions show that weak nonspecific interactions, equivalent to 2−3 peptide hydrogen bonds per 72 nm^2 protein surface area, are enough to counteract depletion to the point where there is only a net crowding effect under highly crowded conditions.

Our model agrees with our experimental results on several important points. We observe associative interactions dominating at low concentrations of crowding agent (Figure 5D), which corresponds to the initial dip in FRET efficiency of the probe. At high concentrations, the probe is saturated and the free energy contribution of associative interactions levels off (Figure 5C). Because depletion free energy continues to decrease linearly (Figure 5B), depletion starts to compensate for associative interactions. The FRET curves measured in BSA and ovomucoid fit this profile. As Ficoll 70 has a very low propensity for associative interactions with the probes, the model prediction for Ficoll 70 crowding would be close to Figure 5B (depletion only). We indeed do not observe the initial dip in FRET efficiency resulting from associative interactions. As we cannot convert free energies of depletion directly to FRET efficiencies, the model provides a qualitative prediction. However, as FRET is proportional to the inverse of the distance between donor and acceptor to the sixth power, we expect the increase in FRET efficiency to follow nonlinearly with respect to an increase in depletion force. We indeed observe a nonlinear increase in FRET efficiency when increasing the Ficoll 70 concentration. The qualitative predictions of our model therefore fit our experiments on BSA and Ficoll 70 crowding.

We also see a clear effect of probe size (Figure 5D): depletion forces are not able to compensate for associative interactions with small probes, while for large probes depletion interactions eventually overcome the free energy barrier of associative interactions. A zoom (Figure S2) shows that for large probes, depletion overcomes associative interactions at ∼15 vol % for while a probe the size of GFP, depletion

DOI: 10.1021/jacs.5b07898
J. Am. Chem. Soc. 2015, 137, 13041−13048

overcomes associative interactions only at ~20 vol %. This fits our observations, as we observe no net depletion effect with a small probe (FRET construct) while a much larger probe (FtsZ) shows strong depletion effects under crowded conditions. Furthermore, the free energy of binding is more sensitive to temperature than depletion in our model (Figure 5E), which fits our observation that FRET efficiencies in BSA are more temperature sensitive than those in Ficoll 70. Our experimental data (Figure 3) and model (Figure 5E) predict that for a certain crowded condition, there can be a crossover temperature where depletion overcomes associative interactions. An increase in temperature could therefore push the balance in favor of the depletion interaction. A similar conclusion was drawn in a theoretical treatment by Zhou[30] of experimental data from the Pielak group[16,26,49] on protein stability under crowded conditions, where they state that "The size, shape, and chemical nature of the crowders determine the relative weights of the two components, but in all cases the net effect is destabilizing below a crossover temperature and stabilizing above it."

What impact do our findings have on the possible role of crowding in the cytosol? As noted by Marenduzzo et al., structures of a size of about 75 nm will theoretically be subjected to ~5k_BT of depletion force, enough for irreversible aggregation.[6] Thus, counteracting forces must be present in the cytosolic environment to prevent all macromolecules from aggregating. Our experimental results and model suggest that whether excluded volume effects are dominant or not, depends on both the size of molecules involved and the strength of associative interactions. Of course, the precise balance between depletion forces and enthalpic interactions depends on the size and shape of the macromolecules, the strength of the specific binding constant, the surface chemistry and the number of nonspecific interactions involved. In our model, we have simplified this picture by taking into account a single nonspecific interaction per a certain amount of surface area of the probe and a fixed, experimentally derived, binding constant.

The picture that emerges is that in the cytosol, depletion forces will only have a minor impact on the interactions between small macromolecules. For monomeric proteins, our experimental results and model suggest that depletion interactions and nonspecific associative interactions balance out almost completely at physiologically relevant conditions (Figures 2 and 5D,E). On a monomeric protein level, this balance avoids dominance of nonspecific interactions (such as depletion and weak associative interactions, which are always present in such crowded environments) over specific, functional interactions. In contrast, large macromolecular (RNA, proteins) complexes as well as fibrillar proteins will increasingly experience the effect of depletion interactions, which at high overlap volumes can overwhelm nonspecific associative interactions with the crowded background. This implies that intracellular macromolecular binding constants are finely tuned to exploit depletion forces while avoiding large scale aggregation.

MATERIALS AND METHODS

***E. coli* Lysate Preparation.** The lysate preparation protocol is based on a number of literature protocols.[50,51] *E. coli* Rosetta2 cells were grown in LB until late-exponential phase (~OD 2.0). After lysozyme treatment, spheroplasts were lysed by ultrasonication. Lysate was recovered by centrifugation and the membrane fraction was removed by ultracentrifugation. The lysate was was dialyzed overnight against MiliQ in dialysis tubing (3.5 kDa cutoff). Lysate was collected and lyophilized in small aliquots. Freeze-dried lysate was stored at −80 °C. See SI Materials and Methods for full protocol.

Reconstitution. High concentrations of lysate were achieved by centrifuging freeze-dried lysate with buffer. Buffer was added to the cake in a volume required to achieve a certain final concentrations. Samples were spun (1000*g*, 2 min, 4°C). Contents were mixed by stirring followed by a long centrifugation step (20 000*g*, 30 min, 4°C). The supernatant was collected as the reconstituted lysate. Protein concentrations were determined by Pierce BCA assay (Life Technologies).

Sample Preparation. Mixtures were prepared in 40 μL volumes in triplicate: 50 mM HEPES pH 7.5; 180 mM potassium glutamate; 10 mM magnesium glutamate; various concentrations of crowding agent; ATeam or DTeam probe. Mixtures were mixed well by pipetting, and 30 μL was loaded on a 384 glass-bottom wells plate (Greiner) and briefly spun on a Eppendorf 5810 R centrifuge.

FRET Measurements. Plates were read on a Tecan Infinite M200 plate reader. Plates were incubated for 10 min at 37°C (unless otherwise specified) before reading. Bottom reading was used, with optimized gain settings. Excitation was set at λ_{ex}= 430 nm (CFP), emission was read at λ_{em} 475 (CFP) and 527 nm (YFP). YFP fluorescence was checked by excitation at λ_{ex} = 515 nm and emission λ_{em} = 550 nm. Triplicate samples were prepared and each sample was measured three times. Measurements were averaged and the averages of three samples provided the average FRET efficiency and standard deviation. Autofluorescence subtraction, absorption correction and in cell measurements are described in SI Materials and Methods.

FtsZ Experiments. FtsZ solution (25 μM *E. coli* FtsZ and 0.25 μM *E. coli* FtsZ-Alexa488 (0.12 μM Alexa488) in 5 mM magnesium glutamate, 180 mM potassium glutamate and 50 mM HEPES buffer pH 7.5) and GTP/crowder solution (6 mM GTP and 187 g/L PEG-8000, Ficoll 70, BSA or ovomucoid, or 50 g/L nondialyzed cell lysate (sept 10 batch) in 5 mM magnesium glutamate, 180 mM potassium glutamate and 50 mM HEPES buffer pH 7.5) are combined on chip and droplets are generated using 25 g/L *E. coli* lipids (Avanti Polar Lipids, Alabaster, AL) in mineral oil. Samples were observed with a spinning disk confocal microscope (CSU-X1, Yokogawa Electric Corp.) on an Olympus inverted microscope (IX81). Alexa-488 was excited with 488 nm laser light (λ_{em} = 525 nm), and images were recorded with a temperature controlled EM-CCD camera (iXon3, Andor) using an exposure time of 0.8−1 s and a piezo-driven 100× (1.3 NA) oil immersion objective. All observations were conducted at room temperature. For full protocol, see the SI Materials and Methods.

For full Materials and Methods, see the Supporting Information.

ASSOCIATED CONTENT

Supporting Information

The Supporting Information is available free of charge on the ACS Publications website at DOI: 10.1021/jacs.5b07898.

Additonal data (Table S1, Figures S1 and S2); full Materials and Methods (PDF)

AUTHOR INFORMATION

Corresponding Author

*w.huck@science.ru.nl

Notes

The authors declare no competing financial interest.

ACKNOWLEDGMENTS

Work in the Huck group was supported by a European Research Council Advanced Grant (246812 Intercom), and VICI (700.10.444) and ECHO-STIP (717.012.001) grants of The Netherlands Organization for Scientific Research. D.F.

DOI: 10.1021/jacs.5b07898
J. Am. Chem. Soc. 2015, 137, 13041−13048

gratefully acknowledges funding from Radboud University (Bionic Cell project). A.J.B. was supported by a VENI grant of The Netherlands Organization for Scientific Research. The Rivas group acknowledges the support of the Spanish Government through Grants BIO211-28941-C03-03 and BFU2014-52070-C2-2-P.

REFERENCES

(1) Fulton, A. B. *Cell* **1982**, *30*, 345.
(2) Zimmerman, S. B.; Trach, S. O. *J. Mol. Biol.* **1991**, *222*, 599.
(3) Golding, I.; Cox, E. C. *Phys. Rev. Lett.* **2006**, *96*, 098102.
(4) Ridgway, D.; Broderick, G.; Lopez-Campistrous, A.; Ru'aini, M.; Winter, P.; Hamilton, M.; Boulanger, P.; Kovalenko, A.; Ellison, M. J. *Biophys. J.* **2008**, *94*, 3748.
(5) Minton, A. P. *J. Biol. Chem.* **2001**, *276*, 10577.
(6) Marenduzzo, D.; Finan, K.; Cook, P. R. *J. Cell Biol.* **2006**, *175*, 681.
(7) Zhou, H.-X.; Rivas, G.; Minton, A. P. *Annu. Rev. Biophys.* **2008**, *37*, 375.
(8) Asakura, S.; Oosawa, F. *J. Polym. Sci.* **1958**, *33*, 183.
(9) Sokolova, E.; Spruijt, E.; Hansen, M. M.; Dubuc, E.; Groen, J.; Chokkalingam, V.; Piruska, A.; Heus, H. A.; Huck, W. T. S. *Proc. Natl. Acad. Sci. U. S. A.* **2013**, *110*, 11692.
(10) Zimmerman, S. B.; Harrison, B. *Proc. Natl. Acad. Sci. U. S. A.* **1987**, *84*, 1871.
(11) del Álamo, M.; Rivas, G.; Mateu, M. G. *J. Virol.* **2005**, *79*, 14271.
(12) Strulson, C. A.; Molden, R. C.; Keating, C. D.; Bevilacqua, P. C. *Nat. Chem.* **2012**, *4*, 941.
(13) Murphy, L. D.; Zimmerman, S. B. *Biophys. Chem.* **1995**, *57*, 71.
(14) Minh, D. D.; Chang, C.-e.; Trylska, J.; Tozzini, V.; McCammon, J. A. *J. Am. Chem. Soc.* **2006**, *128*, 6006.
(15) Totani, K.; Ihara, Y.; Matsuo, I.; Ito, Y. *J. Am. Chem. Soc.* **2008**, *130*, 2101.
(16) Miklos, A. C.; Sarkar, M.; Wang, Y.; Pielak, G. J. *J. Am. Chem. Soc.* **2011**, *133*, 7116.
(17) Stagg, L.; Zhang, S.-Q.; Cheung, M. S.; Wittung-Stafshede, P. *Proc. Natl. Acad. Sci. U. S. A.* **2007**, *104*, 18976.
(18) Ai, X.; Zhou, Z.; Bai, Y.; Choy, W.-Y. *J. Am. Chem. Soc.* **2006**, *128*, 3916.
(19) Charlton, L. M.; Barnes, C. O.; Li, C.; Orans, J.; Young, G. B.; Pielak, G. J. *J. Am. Chem. Soc.* **2008**, *130*, 6826.
(20) Hong, J.; Gierasch, L. M. *J. Am. Chem. Soc.* **2010**, *132*, 10445.
(21) Munishkina, L. A.; Cooper, E. M.; Uversky, V. N.; Fink, A. L. *J. Mol. Recognit.* **2004**, *17*, 456.
(22) Munishkina, L. A.; Ahmad, A.; Fink, A. L.; Uversky, V. N. *Biochemistry* **2008**, *47*, 8993.
(23) Bokvist, M.; Gröbner, G. *J. Am. Chem. Soc.* **2007**, *129*, 14848.
(24) Elcock, A. H. *Curr. Opin. Struct. Biol.* **2010**, *20*, 196.
(25) McGuffee, S. R.; Elcock, A. H. *PLoS Comput. Biol.* **2010**, *6*, e1000694.
(26) Sarkar, M.; Smith, A. E.; Pielak, G. J. *Proc. Natl. Acad. Sci. U. S. A.* **2013**, *110*, 19342.
(27) Sarkar, M.; Li, C.; Pielak, G. *Biophys. Rev.* **2013**, *5*, 187.
(28) Schlesinger, A. P.; Wang, Y.; Tadeo, X.; Millet, O.; Pielak, G. J. *J. Am. Chem. Soc.* **2011**, *133*, 8082.
(29) Minton, A. P. *Biopolymers* **2013**, *99*, 239.
(30) Zhou, H.-X. *FEBS Lett.* **2013**, *587*, 394.
(31) Wang, Y.; Li, C.; Pielak, G. J. *J. Am. Chem. Soc.* **2010**, *132*, 9392.
(32) Boersma, A. J.; Zuhorn, I. S.; Poolman, B. *Nat. Methods* **2015**, *12*, 227.
(33) Gnutt, D.; Gao, M.; Brylski, O.; Heyden, M.; Ebbinghaus, S. *Angew. Chem., Int. Ed.* **2015**, *54*, 2548.
(34) Imamura, H.; Nhat, K. P.; Togawa, H.; Saito, K.; Iino, R.; Kato-Yamada, Y.; Nagai, T.; Noji, H. *Proc. Natl. Acad. Sci. U. S. A.* **2009**, *106*, 15651.
(35) Tadros, M.; González, J. M.; Rivas, G.; Vicente, M.; Mingorance, J. *FEBS Lett.* **2006**, *580*, 4941.
(36) Adams, D. W.; Errington, J. *Nat. Rev. Microbiol.* **2009**, *7*, 642.
(37) Mingorance, J.; Rivas, G.; Vélez, M.; Gómez-Puertas, P.; Vicente, M. *Trends Microbiol.* **2010**, *18*, 348.
(38) Erickson, H. P.; Anderson, D. E.; Osawa, M. *Microbiol. Mol. Biol. Rev.* **2010**, *74*, 504.
(39) Huecas, S.; Llorca, O.; Boskovic, J.; Martín-Benito, J.; Valpuesta, J. M.; Andreu, J. M. *Biophys. J.* **2008**, *94*, 1796.
(40) Mellouli, S.; Monterroso, B.; Vutukuri, H. R.; te Brinke, E.; Chokkalingam, V.; Rivas, G.; Huck, W. T. S. *Soft Matter* **2013**, *9*, 10493.
(41) Yaginuma, H.; Kawai, S.; Tabata, K. V.; Tomiyama, K.; Kakizuka, A.; Komatsuzaki, T.; Noji, H.; Imamura, H. *Sci. Rep.* **2014**, *4*, 6522.
(42) Srere, P. A. *Trends Biochem. Sci.* **1980**, *5*, 120.
(43) Ghaemmaghami, S.; Oas, T. G. *Nat. Struct. Biol.* **2001**, *8*, 879.
(44) Ignatova, Z.; Krishnan, B.; Bombardier, J. P.; Marcelino, A. M. C.; Hong, J.; Gierasch, L. M. *Biopolymers* **2007**, *88*, 157.
(45) Gershenson, A.; Gierasch, L. M. *Curr. Opin. Struct. Biol.* **2011**, *21*, 32.
(46) Latham, M. P.; Kay, L. E. *J. Biomol. NMR* **2013**, *55*, 239.
(47) Sorensen, B. R.; Shea, M. A. *Biophys. J.* **1996**, *71*, 3407.
(48) Sheu, S.-Y.; Yang, D.-Y.; Selzle, H.; Schlag, E. *Proc. Natl. Acad. Sci. U. S. A.* **2003**, *100*, 12683.
(49) Wang, Y.; Sarkar, M.; Smith, A. E.; Krois, A. S.; Pielak, G. J. *J. Am. Chem. Soc.* **2012**, *134*, 16614.
(50) Feilmeier, B. J.; Iseminger, G.; Schroeder, D.; Webber, H.; Phillips, G. J. *J. Bacteriol.* **2000**, *182*, 4068.
(51) Shin, J.; Noireaux, V. *J. Biol. Eng.* **2010**, *4*, 8.

DOI: 10.1021/jacs.5b07898
J. Am. Chem. Soc. 2015, 137, 13041−13048